The Journal of Microbiology, December 1998, p.266-272

Vol. 36, No. 4

Secondary Structure Analysis of Amino Terminal Domain in Phage Lambda Integrase

Jeong-A Yu, Chan-Eun Nam[1], and Eun Hee Cho*

Department of Science Education and
[1]Department of Genetic Engineering, Chosun University, Kwangju 501-759, Korea

(Received October 28, 1998 / Accepted December 8, 1998)

The amino-terminal domain of bacteriophage λ integrase recognizes specific DNA sequences called arm-type sites. To study the structural and functional relationships of the integrase arm-type DNA binding domain, we cloned and purified histidine-tagged amino terminal domains with 64 or 93 amino acid residues of integrase. The DNA binding activities of the histidine-tagged amino terminal domains were confirmed by gel mobility-shift assay. The polypeptides were subjected to circular dichroism spectroscopy to estimate the amount of secondary structures they contain. Based upon analyses of circular dichroism spectra and comparison with predicted secondary structural compositions, it was estimated that the amino terminal domain of integrase in an aqueous solution was composed of a little α-helical region. The helical content increased with an increasing amount of ethanol, an α-helix inducer. This indicates that its conformation can be changed to a form with higher content of α-helical structure under a certain condition.

Key words: Integrase, lambda, arm-Type DNA binding, secondary structure, circular dichroism, DNA binding domain

Bacteriophage λ integrase (Int) is a sequence-specific recombinase which carries out site-specific recombination of λ (15). Int recognizes two distinct classes of DNA sequences, the "core-type" and the "arm-type" binding sites (26, 27). The core-type sites consis of imperfect inverted repeats that flank the sites of strand exchange during recombination. The arm-type sites are characterized by a consensus, C/AAGTCACTAT, which occurs five times outside the region of strand exchange in the phage attachment site, *attP*. Two sites, P1 and P2 are located in the P arm and three contiguous P'1, P'2, and P'3 sites are in the P' arm of the *attP*. Int binding to these arm-type sites, in conjunction with accessary proteins encoded by both the phage and the host, is required to form higher-order nucleoprotein structures, called intasomes, that are necessary for recombination (13, 19).

The Int protein of λ is the best-characterized member of an integrase family of tyrosine recombinases (8, 22). Crystal structure of a minimal catalytic domain containing residues from 170 to 356, the region that the λ Int shares high level of similarities with other members of the integrase family, was revealed recently (14). However, a few analyses have been carried out to study Int recognition to the arm-type binding sites. Mutational analysis of arm-type sites indicates that most base pairs in the conserved sequence are important in sequence-specific recognition of the Int protein (16) and partial proteolytic study shows that amino terminal domain of 64 amino acid residues carry the arm-type binding specificity (21). Int has no obvious helix-turn-helix motif or any other DNA binding motif that is characteristic of sequence-specific DNA binding proteins (6, 32). The arm-type binding sites are also unique in that they are arranged in tandem repeats rather than in inverted repeats as shown in most of the other protein recognition sites. Thus the arm-type DNA binding domain of λ Int may contain a novel type of sequence-specific DNA binding motif.

To study the structure and functional relationships of the Int arm-type binding domain, we cloned the regions of the int gene encoding amino terminal 64 or 93 amino acid residues fused with a polypeptide containing six histidine residues. We confirmed that the His-tagged truncated Int polypeptides retained their ability to recognize arm-type sequences by gel molibity shift assays. Those polypeptides were subjected to circular dichroism (CD) spectrometric analyses to detemine the secondary structural compositions of the Int amino-terminal domain.

* To whom correspondence should be addressed.
(Tel) 062-230-7370; (Fax) 062-232-8122
(E-mail) ehcho@chosun.ac.kr

Materials and Methods

Media, chemicals, and enzymes

Luria-Bertani (LB) medium (tryptone, 10 g/l; yeast extract, 5 g/l; NaCl, 5 g/l) was used as a rich medium. Kanamycin sulfate and Isopropyl-β-*D*-thiogalactoside (IPTG) were supplemented to the medium to a final concentration of 40 μg/ml and 1 mM, respectively, when ever needed. *Taq* DNA polymerase was obtained from Promega. Restriction enzymes and DNA modifying enzymes were purchased from Promega or New England Biolabs.

Cloning of His-tagged amino terminal domain of λ int

Polymerase Chain Reaction (PCR) was carried out with 1 unit of *Taq* polymerase in 10 mM Tris-HCl (pH 8.3), 50 mM KCl, 1.5 mM $MgCl_2$, 0.01% gelatin, 200 uM deoxynucleoside triphosphate, 10 ng of plasmid DNA, pSX1-2, containing λ *int* gene, and 20 pmole of primers (16). The upstream primer (AGAGGATCACATATGGGAAGAAGGCGAAGTC) contained the *Nde*I restriction site overlapping with the initiation codon of the *int* gene. Two kinds of downstream primers were used to amplify different lengths of the *int* gene. One (ATCACTGTTGAATTCTCGCTTACAGAGGCTTGTGTTTGTG) contained an ochre codon at 65th position and the other (TTTGTTGCAACGAATTCAGGTCACTATCAGTC) contained an amber codon at 94th position followed by an *Eco*RI site. The *Nde*I-*Eco*RI fragment of the amplified product was ligated with the plasmid pET28a (Novagene) which was pretreated with enzymes *Nde*I and *Eco*RI. After transformation into an *E. coli* strain DH5α (*supE44, ΔlacU169*(φ80 *lacZ* ΔM15), *hsdR17, recA1, endA1, gyrA96, thi-1, relA1*), the clones harboring each fragment were confirmed by the method of chain termination (31). The clones, pHis-Int64 carrying int65 (och) and pHis-Int93 with int94 (amb), were electrotransformed into *E. coli* BL21 (DE3) (F^-, *ompT*, *hsdSb*($r_B^- m_B^-$), *gal*(λ *cI857, ind1, Sam7, nin5, lacUV5-T7 gene1*), *dcm*) for further studies.

Expression and purification of His-tagged int arm-type DNA binding domain

E. coli strain BL21 (DE3) containing a plasmid, pHis-Int64 or pHis-Int93, was grown to an exponential phase in LB medium with kanamycin selection. The expression of amino terminal domains was induced by adding 1 mM IPTG in a final concentration. After 3 hours of induction, cells were collected by centrifugation and disrupted by sonication in 50 mM Na-phosphate buffer (pH 7.4) with 300 mM NaCl and 10% glycerol. Sonicated samples were centrifuged and the supernatants were saved. The sonic extracts were applied onto an Ni^+-NTA column (Qiagene) and washed extensively with the sonication buffer containing 40 mM imidazole. The His-tagged Int amino terminal domain was eluted with 250 mM imidazole in sonication buffer. Protein concentrations were determined by dye-binding assays (3).

Gel mobility shift assays

A 160 bp fragment with P' arm was synthesized by PCR from P22 challenge phage P'123(II) which carries P'1, P'2, and P'3 sites of λ and a 174 bp fragment without Int binding sites was synthesized from the challenge phage P224B (16). Synthetic oligonucleotides (CGGCATTTTGCTATTCC and GATCATCTAGCCATGC) were used as primers for amplification. One of the primer was labeled prior to use with [γ-^{32}P]ATP and T4 polynucleotide kinase (30).

Aliquots of labeled DNA fragments were incubated with various concentrations of the His-Int64 or His-Int93 in binding buffer (44 mM Tris-HCl, pH 8.0, 66 mM KCl, 0.5 mg/ml Bovine Serum Albumin, 5 mM EDTA, 5 mM spermidine, 11 mM borate, 10% glycerol, 5 μg/ml sonicated calf thymus DNA) at room temperature for 30 min. The final reaction volume was adjusted to 10 μl. After electrophoresis on 5% polyacrylamde gels at 4°C, the gel was dried and analyzed using PhosphorImager (Molecular Dynamics).

Circular dichroism spectroscopy

Circular dichroism (CD) spectra were obtained with a Jasco 715 spectropolarimeter at 25°C using a quartz cylindrical cell in 0.1 cm path length. The spectra were recorded from 190 nm to 260 nm and averaged to 10 scans at 0.5 nm resolution. Protein concentrations ranged from 67 μg/ml to 266 μg/ml in 50 mM phosphate buffer (pH 7.4) containing 60 mM KCl in aqueous solution or in buffer/ethanol mixture. Buffer base lines were subtracted and smoothed by a 13-point quadratic-cubic function. The resulting spectra were analyzed using programs CDFIT and K2d which allowed the data to be filted to three standard conformations (α-helix/β-sheet/coil). The former method fits data to be analyzed to the standards by the method of least-squares using the reference data of Greenfield and Freedman (11). The latter uses a Neural network methods using 18 proteins with known X-ray crystal structures (20). For the secondary structure fit the molecular weight of 10,080 and 13,560 g/mol were used for His-Int64 and His-Int93, respectively. All spectra were presented in CD (mdeg; $3300[A_L-A_R]$) instead of in mean residue ellipticity [θ] (deg cm^2 $dmol^{-1}$). [θ] can be caculated by using the relationship; [θ]=100 CD/cnl where c is the peptide concentration (mM), n is the number

of amino acids in the peptide, and l is the path length (cm) (17).

Secondary structure predictions

Secondary structures of the polypeptides, His-Int64 and His-Int94, were predicted on the basis of the amino acid sequences by using methods available in the world wide web. PHD program (28, 29) was obtained at the PredictProtein Server (http://www.embl-heidelberg.de/predictprotein/predictprotein.html). Also used algorithms such as Predator (1), Gor IV (9), SOPMA (10), DPM (5), and LEVIN (18) were obtained at Network Protein Sequence analysis at IBCP, France (http://pbil.ibcp.fr/).

Results and Discussion

The minimum domain of λ Int protein which shows arm-type DNA binding specificity is the polypeptide composed of the first 64 amino acids (21). An amber mutant, *int(am)94*, which expresses the amino termial 93 amino acids was first isolated by Bear *et al.* (2), and was subsequently shown to contain arm-type binding affinity *in vivo* (12). In this study, we analyzed and compared secondary structures of these two truncated amino terminal parts of Int protein.

The *int* gene of λ was cloned under T7 promoter control in such a way that amino terminal 64 or 93 amino acid residues were fused with a polypeptide of 20 amino acids in length containing six consecutive histidine residues. PCR was carried out to amplify part of the ιντ gene which can express amino terminal domains in two different lengths. The PCR reaction yielded DNA fragments of approximately 210 bp and 240 bp, corresponding to the sizes predicted from the nucleotide sequences. The amplified products were cloned into the plasmid pET28a(+). Sequencing analyses of cloned fragments confirmed that the amino termini of both clones were properly fused to the polypeptide containing six histidine residues. We also identified the introduction of the ochre codon at 65th position of the int gene in the plasmid pHis-Int64 and the amber codon at 94th position in the plasmid pHis-Int93. The cloned plasmids, pHis-Int64 and pHis-Int93, were introduced to an *E. coli* strain BL21 (DE3), where the His-tagged polypeptides were expressed.

After polypeptide expression, the cell-free extracts were loaded onto Ni^{+}-NTA column and the His-tagged Int amino terminal polypeptides were eluted by addition of imidazole in discontinuous concentration gradients. Majority of the His-tagged Int64 was eluted by 200 mM imidazole, and the remaining polypeptide was eluted by 300 mM imidazole (Fig. 1a). Based upon these results, His-Int64 and His-Int93 polypeptides were eluted by addition of 250 mM imidazole in subsequent experiments (Fig. 1b and c).

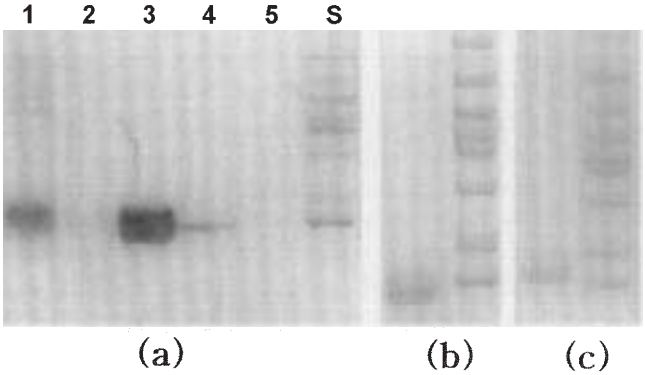

Fig. 1. Purification of histidine-tagged Int amino terminal domains. (a) Purification of His-Int64 from BL21(DE3)/pHis-Int64. Crude exctracts were loaded on lane 1 and fractions eluted with discontinuous imidazole gradients dissolved in 50 mM sodium phosphate (pH 7.4), 300 mM NaCl, 10% (w/v) glycerol were shown lanes 2 (100 mM imidazole), 3 (200 mM imidazole), 4, (300 mM imidazole) and 5 (400 mM imidazole). (b) Purified His-Int64. (c) Purified His-Int93. Molecular weight standards used on these gels are Mid-range markers (Promega); Phophoylase B, 97.4 kD; BSA, 66.2 kD, Glutamate dehydrogenase, 55.0 kD; Ovalbumin, 42.7 kD; Aldolase, 40.0kD; Carbonic anhydrase, 31.0 kD; Soybean Trypsin inhibitor, 21.3 kD; Lysozyme, 14.4 kD.

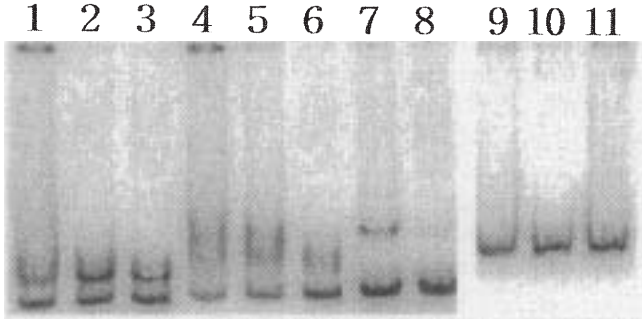

Fig. 2. Gel mobility shift assays of DNA fragments containing the arm-type binding sites. Various concentrations (4 μM polypeptides in lanes 1 and 4; 2 μM in lanes 2 and 5; 1 μM in lanes 3 and 6) of His-Int64 (lanes 1, 2, and 3) and His-Int93 (lanes 4, 5 and 6) were incubated with labeled DNA containing the arm-type binding sites, P'1, P'2, and P'3. Lane 7 contained 0.5 μM of His-tagged full length Int protein and DNA fragments with the arm-type binding sites. Lane 8 represents free fragments containing the arm-type binding sites with no protein added. Lanes 9 to 11 represent gel binding reactions in which proteins were incubated with labeled DNA without Int binding sites (2 μM His-Int64 in lane 9; 2 μM His-Int93 in lane 10; no protein in lane 11). All the reactions carried sonicated calf thymus DNA in final concentration of 5 μg/ml as a non-specific competitor.

The arm-type binding activity of the purified His-tagged Int amino terminal domains was measured by gel mobility shift assays (Fig. 2). If the His-tagged polypeptides retain arm-type binding specificity, we can directly use the fusion proteins to assess secondary structural composition of the arm-type DNA binding motif. The labeled DNA fragments contain three consecutive arm-type sites, P'1, P'2, and P'3 sites, of P' arm on the *attP* and *attL* sites. Within a range of 1 μM to 4 μM of His-Int64 and His-Int93, the specific protein-DNA complexes were detected when the nonspecific competitor DNA was added in 10~20 fold excess to the specific DNA (Fig. 2, lanes 1-8). When the nonspecific DNA of similar length was labeled and used as a templates, protein-DNA complexe the were not observed (Fig. 2, lanes 9-11). This indicated that the His-Int64 and His-Int93 carried arm-type DNA binding specificity even when the trucated Int amio terminal regions were fused with a leader polypeptide containing histidines. Therefore, we decided to use these His-tagged polypeptides for the secondary structural analyses of the Int arm-type DNA binding domain.

CD spectra of the His-Int64 and His-Int93 were obtained to estimate the secondary structural composition of the Int arm-type binding domain. Polypeptide His-Int93 showed similar CD spectra independent of its concentrations between 67 μg/ml and 266 μg/ml. However, the CD spectra of His-Int 64 were highly dependent on its concentrations locating negative minimum between 210 nm and 220 nm spectral region when concentrations of the polypeptide were higher than 177 μg/ml (data not shown). This suggests that His-Int64 at high concentrations did not form any particular secondary structures rather it showed the beta aggregation characteristic of the His-Int64 (25). Below 133 μg/ml of His-Int64, CD profiles fluctuated within a resonable range, and at 133 μg/ml the signal to noise ratio was high enough to do the data fit.

At the concentration of 133 μg/ml, both the polypeptides, His-Int64 and His-Int93, showed CD spectra with a strong negative band between 208 nm and 219 nm (Fig. 3). Based on the analyses using CDFIT, His-Int64 in aqueous solution was estimated to contain 12% α-helix, 42% β structure, and 46% random coils, and His-Int93 to contain 13% α-helix, 39% β structure, and 48% random coil structures. The fitted data of His-Int93 were in relatively good agreement with the experimental data with small residue (<8%), however those of His-Int64 showed large remainder (~20%) in the spectral region between 205 nm and 215 nm and below 200 nm. A typical helical structure shows a well defined negative double minimum at 208 nm

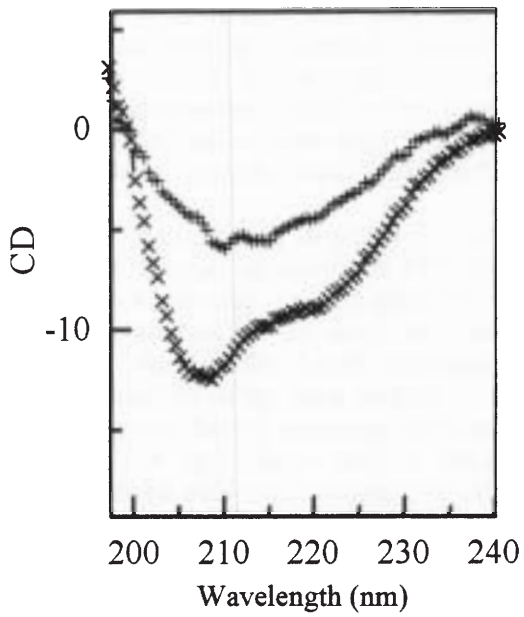

Fig. 3. UV-CD spectra of polypeptides His-Int64(+) and His-Int93 (×). CD spectra were obtained in 50 mM phosphate buffer (pH7.4) containing 60 mM KCl at 25°C. The buffer base line was subtracted and smoothed. The spectra were presented in CD (mdeg; 3300[AL-AR]) instead of in mean residue ellipticity [θ](deg cm^2 dmol $^{-1}$).

Fig. 4. Secondary structure of His-Int93 predicted by various computer algorithms. h=helix; e=extended sheet; t=turn; c, s=coil; ?=ambiguous. Consensus represents the strucuture which is predicted by more than four methods out of six. The region where all computer modelling methods used in this study predicted α-helical structure was marked by two filled down-triangles (▼). ▽ indicates the initiation codon of Int protein in the absence of the His-tag leader peptide.

and 220 nm (33). The results from the data fit of the His-Int64, showed large deviation only below 215 nm, implying that the helical composition of 12% could have been overestimated. We used another fitting algorithm, called K2d (20), and the results from K2d were similar to those from the CDFIT.

In terms of α-helical composition, the estimated values by CD spectroscopy agreed relatively well with those predicted by protein secondary structure prediction from the amino acid sequences. In the polypeptide His-Int93, amino acid residues from 45 to 52 and from 80 to 88 were predicted to form α-helical structure by all six prediction programs used in this study (Fig. 4). This indicates that these two regions are very likely to form helical structures in the His-Int93. This matches well with the value of 10~15% which was calculated to form α-helical structures in CD spectrophotometry. When the first 64 amino acid sequences along with those of the leader peptide were given, the predicted secondary strucutres by all the six methods were almost as same as shown in Fig. 5 except that the α-helical region became a little shorter and was positioned between amino acid residues 47 and 50. Considering the possibily that 12% of helical composition of His-Int64 in CD measurement may have been overestimated, this region may be the only region forming a helical structure. On the basis of these results, we concluded that the amino-terminal domain of the λ integrase which is composed of the amino terminal 64 amino acids contained a single α-helix spanning amino acid residues approximately from 45 to 50.

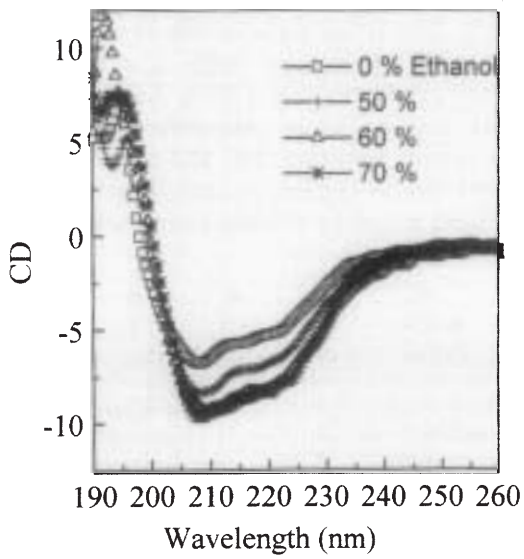

Fig. 5. UV-CD spectra of His-Int93 at various ethanol concentrations. Spectra of 67 μg/ml His-Int93 were obtained at various volume% of ethanol over 50 mM phosphate buffer (pH 7.4) containing 60 mM KCl.

On the other hand, the amounts of β-conformation varied greatly depending on prediction methods. While β-structure contents in the His-Int 64 and the His-Int93 which were obtained from CD spectra were approximately 40%, the predicted values based on amino acid sequences were only about 10%. It has been considered that CD spectrometric analyses are not as good in estimating β-structure composition as in α-helical contents (33, 34). Moreover, the known prediction accuracies of β-structure in computer modeling used in this study are lower than those of α-helix (1, 5, 9, 10, 18). Thus it was not feasible to predict β-structural composition based upon these results.

We next examined the effects of hydrophobic environment on the secondary structural contents by measuring the CD spectrum of the polypeptides in water/ethanol mixture. By increasing the composition of ethanol, a known helix inducer (4, 7), the CD spectra of His-Int93 showed progressive increase in the negative minima between 208 and 222 nm, with well defined isometric point at 203 nm which indicates an equilibrium between two conformations (Fig. 5). The amount of α-helix in the polypeptide increased as the aqueous buffer was gradually substituted with increasing amount of ethanol and was saturated at 60 volume% of ethanol. At a concentration of 67 μg/ml His-Int93, the helical contents were calculated to be 15% in aqueous solution, 22% at 50% ethanol, 28% at 60%, and 29% at 70% ethanol concentrations. This indicates that a conformational change in His-Int93 can be induced under a certain condition. However, His-Int64 in solvents of water/ethanol mixture became rapidly insoluble under same experimental conditions. We were unable to assess the effects of hydrophobic solvent on His-Int64 conformation.

Based on these CD spectroscopic analyses, we concluded that the amount of α-helical structures in the Int arm-type binding domain fragment was very low in aqueous solution. The most likely region to form an α-helical structure was proposed to be the part including amino acid residues 47 to 50 of Int protein. In the presence of an α-helix inducer, the α-helical content increased up to 28%. This indicates that the amino terminal domain of the Int protein has a potential to change its conformation to a form with more helical structure when its local environment is changed. In the cases of some other sequence-specific DNA binding proteins, presence of specific DNA results in an altered conformation of the protein with an increased α-helical content (23, 24).

Acknowledgments

We thank Anca Segall for the generous gift of purified His-tagged Int protein and Jeffrey Gardner for allowing EHC for carrying out gel shift assays in his laboratory. We are grateful to Jung Sub Lee and Moonjoo Koh for critical reading of the manuscript.

This study was supported by the Academic Research Fund (GE96-155) of the Ministry of Education, Republic of Korea.

References

1. **Argos, P. and D. Frishman.** 1996. Incorporation of nonlocal interactions in protein secondary structure prediction from the amino acid sequence. *Protein Eng.* **9**, 133-142.
2. **Bear, S.E., J.B. Clemens, L.W. Enquist, and R.J. Zagursky.** 1987. Mutational analysis of the lambda *int* gene: DNA sequence of dominant mutations. *J. Bacteriol.* **169**, 1880-1883.
3. **Bradford, M.M.** 1976. A rapid and sensitive method for the quantitation of microgram quantities of protein utilizing the principle of protein-dye binding. *Anal. Biochem.* **72**, 248-253.
4. **Conio, G., E. Patrone, and Brighetti.** 1970. The effect of aliphatic alcohols on the helix-coil transition of poly-L-ornithine and poly-L-glutamic acid *J. Biol. Chem.* **245**, 3335-3340.
5. **Deleage, G. and B. Roux.** 1987. An algorithm for protein secondary structure prediction based on class prediction. *Protein Eng.* 1, 289-294.
6. **Dodd, L.B. and J.B. Egan.** 1987. Systematic method for the detection of potential Cro-like DNA-binding region in proteins. *J. Mol. Biol.* **194**, 557-564.
7. **Dufour, E. and T. Haertle.** 1990, Alcohol-induced changes of beta-lactoglobulin -retinol-binding stoichiometry. *Protein Eng.* **4**, 185-190.
8. **Esposito, D. and J.J. Scocca.** 1997. The integrase family of tyrosine recombinases: evloution of a conserved active site domain. *Nucleic Acids Res.* **25**, 3605-3614.
9. **Garnier, J., J.-F. Gibrat, and B. Robson.** 1996. GOR: Secondary structure prediction methods version IV, p. 540-553. *In* R. F. Doolittle (ed.), *Methods in Enzymol.* **266**, Academic Press, Inc., New York.
10. **Geourjon, C. and G. Deleage.** 1995. SOMPA: Significant improvement in protein secondary structure prediction by consensus prediction from multiple alignments, *CABIOS* **11**, 681-684.
11. **Greenfield, N. and G.D. Fasman.** 1969. Computed circular dichroism spectra for the evaluation of protein conformation. *Biochemistry* **8**, 4108-4115.
12. **Han Y.W., R.I. Gumport, and J.F. Gardner.** 1994. Mapping the functional domains of bacteriophage lambda integrase protein. *J. Mol. Biol.* **235**, 908-925.
13. **Kim, S., L. Moitoso de Vargas, S.E. Nunes-Duby, and A. Landy.** 1990. Mapping of a higher order protein-DNA complex: two kinds of long-range interaction in λ *attL*. *Cell* **63**, 773-780.
14. **Kwon, H.J., R. Tirumalai, A. Landy.** 1997. Flexibility in DNA recombination: structure of the lambda integrase catalytic core. *Science* **276**, 126-131.
15. **Landy, A.** 1989. Dynamic, structural, and regulatory aspects of site-specific recombination. *Ann. Rev. Biochem.* **58**, 913-950.
16. **Lee, E.C., R.I. Gumport, and J.F. Gardner.** 1990. Genetic analysis of bacteriophage integrase interactions with arm-type attachment site sequences. *J. Bacteriol.* **172**, 1529-1538.
17. **Lehrman, S.R, J.L. Tuls, and M. Lund.** 1990. Peptide α-helicity in aqueous trifluorethanol: Correlations with predicted α-helicity and the secondary structure of the corresponding regions of Bovine Growth Hormone. *Biochemistry* **29**, 5590-5596.
18. **Levin, J.M. and J. Garnier.** 1986. Improvements in a secondary structure prediction method based on a search for local sequence homologies and its use as a building tool. *Biochim. Biophys. Acta* **955**, 283-295.
19. **MacWilliams, M.P., R.I. Gumport, and J.F. Gardner.** 1996. Genetic analysis of the bacteriophage λ *attL* nucleoprotein complex. *Genetics* **143**, 1069-1079.
20. **Merelo, J.J., M.A. Andrede, A. Prieto, and F. Moran.** 1994. Proteinotopic Feature Maps. *Neurocomputing* **6**, 443-454.
21. **Moitoso de Vargas, N., C.A. Pargellis, N.M. Hasan, E.W. Bushman, and Landy, A.** 1988. Autonomous DNA binding domains of integrase recognize different sequence families. *Cell* **54**, 923-929.
22. **Nunes-Duby, S.E., H.J. Kwon, R.S. Tirumalai, T. Ellenberger, and A. Landy.** 1998. Similarities and differences among 105 members of the Int family of site-specific recombinases. *Nucleic Acids Res.* **26**, 391-406.
23. **O'Neil, K.T., J.D. Shuman, C. Ampe, and W.F. DeGrado.** 1991. DNA-Induced incerase in α-helical content of C/EBP and GCN4. *Biochemistry* **30**, 9030-9034.
24. **Patel, L., C. Abate, and T. Curran.** 1990. Altered protiein conformation on DNA binding by Fos and Jun. *Nature* **347**, 572-574.
25. **Perutz, M.F., T. Johnson, M. Suzuki, and J. Finch.** 1994. Glutamine repeats as polar zippers: Their possible role in inherited neurodegenerative diseases. *Proc. Natl. Acad. Sci., USA* **91**, 5355-5363.
26. **Ross, W. and A. Landy.** 1982. Bacteriophage int protein recognizes two classes of sequence in the phage *att* site: characterization of arm-type sites. *Proc. Natl. Acad. Sci. USA* **79**, 7724-7728.
27. **Ross, W. and A. Landy.** 1983. Patterns of Int recognition in the regions of strand exchange. *Cell* **33**, 261-272.
28. **Rost, B. and C. Sander.** 1993. Prediction of protein structure at better than 70% accuracy. *J. Mol. Biol.* **232**, 584-599.
29. **Rost, B. and C. Sander.** 1994. Combining evolution information and neural networks to predict protein secondary structure. *Proteins* **19**, 55-72.
30. **Sambrook, J., E.F. Firtsch, and T. Maniatis.** 1989. *In* Molecular cloning: a laboratory manual, 2nd ed. Cold Spring Harbor Laboratory Press, Cold Spring Harbor, NY, USA.
31. **Sanger, F., S. Nicklen, and A. Coulson.** 1977. DNA sequencing with chain terminating inhibitors. *Proc. Natl.*

Acad. Sci. USA **74**, 5463-5476.
32. **Steitz, T.A.** 1990. Structural studies of protein-nucleic acid interaction: the sources of sequence-specific binding. *Quart. Rev. Biophy.* **23**, 205-280.
33. **Woody, R.W.** 1995. Circular dichroism, p. 35-71. *In* J.N. Abelson, and M.I. Simon. (eds.) *Methods in Enzymol.*, vol. 246, Academic press, Inc., New York.
34. **Yang, J.T., C.-S.C. Wu, H.M. Martinez.** 1986. Calculation of protein conformation from circular dichroism, p. 208-269. *In* C. H.W. Hirs and S.N. Timasheff (eds.) *Methods in Enzymol.*, vol. 130, Academic press, Inc., New York.